Eur. Phys. J. C 49, 169–175 (2007)
DOI 10.1140/epjc/s10052-006-0091-8

THE EUROPEAN PHYSICAL JOURNAL C

Regular Article – Experimental Physics

The HFT, a Heavy Flavor Tracker for STAR

A. Shabetai[a] for the STAR Collaboration

Institute Pluridisciplinaire Hubert Curien (IPHC), 23 rue de loess, BP 28, 67037 Strasbourg, France

Received: 10 August 2006 /
Published online: 28 November 2006 –

Abstract. Determining the degree of termalisation of the medium created in heavy ion collisions at RHIC remains highly debated. Elliptic flow (v_2) measurements at RHIC have already suggested the development of collectivity among partons before hadronization. If heavy flavor hadrons flow with the light flavor hadrons, this indicates frequent interactions between the light (u, d ,s) and heavy (c, b) quarks. Thus, thermalization of light quarks is likely to have been reached through partonic re-scattering. Experimentally this can be probed by making a direct measurement of D-mesons v_2 with sufficient precision at low transverse momentum. Using the Heavy Flavor Tracker (HFT) detector, the STAR experiment at RHIC is proposing to both study this process and also to directly reconstruct charmed hadrons (D^0, D^+, D_s, Λ_C, ...), using the displaced vertices of their decay products. The HFT is the first vertex detector to use a new and promising CMOS active pixel sensor technology. It will allow to build a relatively fast, accurate and radiation tolerant detector, while keeping the material budget low ($\sim 0.3\% X_0$ per layer). Detector design and physics performance simulations are presented.

1 Introduction

Over the past few years, the Relativistic Heavy Ion Colider (RHIC) has been revealing interesting phenomena produced in relativistic heavy-ion collisions. Among many observations, the suppression of high p_{T} hadrons [1], the elliptic flow (v_2) measurements of multistrange hadrons [2] and the overall agreement of particle ratios with thermal models [3] suggest that the medium created in ultra relativistic collisions is consistent with a highly dissipative matter with partonic degrees of freedom: the quark–gluon plasma (QGP). However, thermalization needs to be fully addressed and many open questions are still to be answered in order to fully describe the properties of this medium. The study of heavy flavors (c and b) properties will provide valuable information for our understanding of the medium created at RHIC.

Heavy quarks are mainly produced by hard processes: gluon fusion and $q\overline{q}$ annihilation. Consequently they are sensitive to early stages of the collision. Heavy quark production is also sensitive to the parton distribution function.

Unlike the light quarks, heavy quark masses are much higher than the initial excitation of the system ($M_c \simeq 1.5\,\mathrm{GeV} \gg \Lambda_{\mathrm{QCD}} \gg M_{ud}$). Their mass structure is unique: quarks are elementary particles and, depending on the energy scale, their mass is generated by two distinct mechanisms: current quark masses are generated by the electroweak symmetry breaking mechanism (Higgs mass) while the spontaneous chiral symmetry breaking of quantum chromo dynamics (QCD) leads to the constituent quark masses. The QCD interaction dominates light quarks (u, d, s) masses, while the heavy quark masses (c, b, t) are mainly produced by the Higgs mechanism, see Fig. 1. If chiral symmetry is restored, they will remain heavy.

These differences between light and heavy quarks make heavy quarks a good probe to study the properties of the hot and dense medium created in high-energy nuclear collisions. The study of heavy flavors has already started at RHIC. Three types of measurements are now ongoing. The first is indirect, measuring the inclusive single electron/positron, spectra [5] (with $1 < p_{\mathrm{T}} < 10\,\mathrm{GeV}/c$) from charm (and beauty) hadron semi-leptonic decays ($(c, b) \to e^- + X$) at $\sqrt{s_{NN}} = 200\,\mathrm{GeV}$. Very low p_{T} single muons ($D^0 \to \mu^+ + X$) are also measured. And finally the Solenoidal Tracker at RHIC [6] (STAR) obtained the first results of directly reconstructed D^0 meson production via its hadronic decay channel [7,8] $D^0 \to K\pi$ with p_{T} up to $3\,\mathrm{GeV}/c$ in minimum bias Au + Au collisions from the same data set, using an event-mixing resonance technique, resulting in a very big residual combinatorial background and, a very small signal over background ratio ($S/B \simeq 1/800$).

When direct measurements of heavy flavor hadrons are not possible, non-photonic electrons from heavy flavor decays can be used to study charm production. However, there are serious limitations in such situations. Electrons are indirect probes. It is not possible to accurately separate e^- coming from D-mesons from those coming from B-mesons. In addition, due to the decay kinematics and

[a] e-mail: shabetai@in2p3.fr

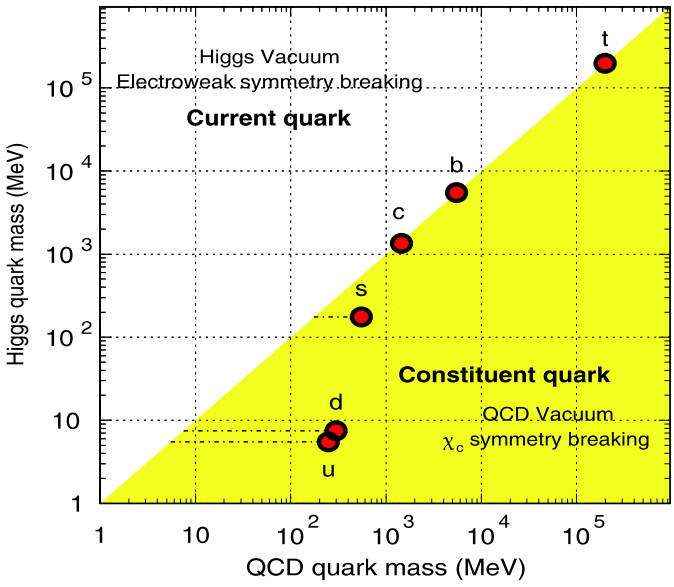

Fig. 1. Quark masses in QCD vacuum and Higgs vacuum. A large fraction of the light quark masses is due to the chiral symmetry breaking in the QCD vacuum. Values of quark masses taken from [4]

the light mass of e^+ and e^-, the dynamical information in the primary spectrum is lost to a large part (especially in the low p_{T} region). The decay electron p_{T} distributions are not directly related to the intrinsic shape of the D-meson transverse momentum distribution. A correlation exists, but is very broad in p_{T}, knowing that the low p_{T} region is essential to check QCD predictions.

Understanding precisely the charm cross-section (expected to follow the binary collision (N_{bin}) scaling from $p+p$, $d+Au$ to Au + Au collisions at RHIC energies [9]) is not easy using indirect probes, but is a key element for understanding QGP properties. One can extract 90% of the total charm yield by directly measuring D-mesons (up-to 3 GeV/c in $d+$Au collisions), but only 15% of this yield is carried by electrons [7, 8] (measured up to 5 GeV/c, in Au + Au collisions).

Due to the high mass and relatively small interaction cross section of heavy quarks, the strength of elliptic flow of heavy flavor hadrons may be a good indicator of thermalization occurring at the partonic level. If heavy flavor hadrons flow together with the light flavor hadrons, this indicates frequent interactions between the light and heavy quarks. Hence, thermalization of light quarks is likely to have been reached through partonic re-scattering. Experimentally the first indication of charm hadron v_2 at RHIC is measured [10] in the inclusive electron channel. Data support the idea that the heavy charm quarks flow, although systematic uncertainties are quite large, especially at low transverse momentum where hydrodynamic behavior should occur. This is mainly due to the photonic background ($\gamma \to e^+ + e^-$) produced in detectors materials (important in STAR case). A precise measurement of directly reconstructed open charm hadrons to low momentum, where the correlation between the electron momentum and the D-meson momentum is weak, is essential to confirm and quantify elliptic flow of the charm quarks and to check theoretical predictions.

The discovery of a factor of 4 to 5 suppression of high p_{T} hadrons ($5 < p_{\mathrm{T}} < 10$ GeV/c) produced in Au + Au collisions at RHIC and the disappearance of the away-side jet has been interpreted as evidence for jet quenching [1]. This effect was predicted to occur due to radiative energy loss of high energy partons that propagate through a dense and strongly interacting medium. Even adding the contribution of elastic processes (collisional energy loss [11]), doesn't seem to be sufficient to precisely predict and understand the energy loss mechanisms, and to match the measured non-photonic electron R_{AA} spectra ($R_{AA}(p_{\mathrm{T}}) = (\mathrm{d}N^{AA}/\mathrm{d}p_{\mathrm{T}})/(\langle T_{AA}\rangle \mathrm{d}\sigma^{pp}/\mathrm{d}p_{\mathrm{T}})$) from RHIC [5] suppressed at high p_{T}. In addition, the relative contribution of D-mesons and B-mesons in this spectra (favor dependence of energy loss) can not be addressed by current measurements. A more accurate energy loss measurement may then be helpful.

Consequently, in order to extract precise information about heavy flavor production in heavy ion collisions, we must measure the charm and beauty-hadrons by direct topological reconstruction, (see Sect. 2). In the present article, we will first describe the device that we are proposing to build in order to make those direct topological measurements (mechanical design, choice of technology and required performances). Afterwords, in Sect. 3, we will discuss some simulation results evaluating the expected performances of this device.

2 The Heavy Flavor Tracker: a new detector concept

To address the currently open questions, the STAR collaboration is proposing [12] to build a new silicon vertex detector (developed by the Lawrence Berkeley National Laboratory).

2.1 Mechanical design

The Heavy Flavor Tracker (shown in Fig. 2) consists of two layers of silicon detectors located very close to the beam pipe. In the current design, this device is surrounded by the Silicon Strip Detector [13] (one layer of strips called SSD) itself surrounded by the STAR Time Projection Chamber [14] (TPC).

Our goal being to measure charmed hadron decays and elliptic flow in the charm sector, the HFT must be able to be efficient down to very low transverse momentum. To acheive this goal, a very thin and precise detector is required.

As we shall show in detail in this section, the STAR running environment, and its heavy flavor physics program require an accurate (detector resolution $\simeq 10\,\mu$m), thin (260 μm equivalent Si per layer), relatively fast (the prototype runs with 4 ms of integration time) detector

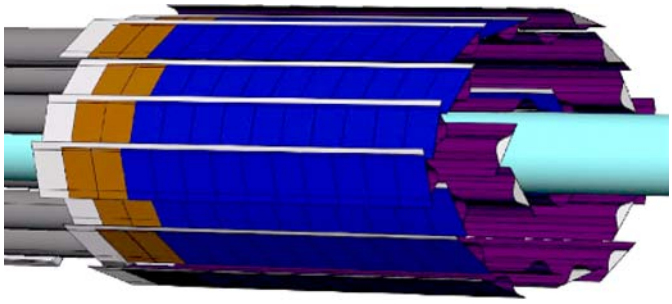

Fig. 2. A drawing of the HFT (side view) surrounding the STAR beam pipe

($\sim 0.4 \times 10^6$ pixels per sensor), able to operate in a relatively high radiation environment.

The proposed HFT aims at improving the single track pointing accuracy of STAR by a factor of ~ 50 and thus allow us to measure very short-lived ($c\tau = 123\,\mu$m for the D^0) particles (see Fig. 3).

The innermost layer of the detector lies at a mean radius of 1.5 cm and is composed of 6 detector ladders. The outer layer lies at a mean radius of 5.0 cm and is composed of 18 ladders. Each ladder contains a row of 10 monolithic CMOS (see Sect. 2.2) detector chips and has an active area of 19.2 cm $\times$ 1.92 cm. Each CMOS detector chip contains 640×640 square pixels (30 μm pitch) and is thinned down to a thickness of 50 μm to minimize multiple coulomb scattering in the detector. The effective thickness of each ladder is 0.28% X_0 of radiation length. For the same reason, the detector will be air-cooled. Bringing the detector to 1.5 cm radius will require a new, smaller radius, beam pipe, this will give the opportunity to make it thinner (0.5 mm).

In recognition of difficulties encountered in a variety of experiments, we are adopting design requirements for rapid insertion and removal of the vertex detector, rapid calibration and we are planning to build multiple detector copies.

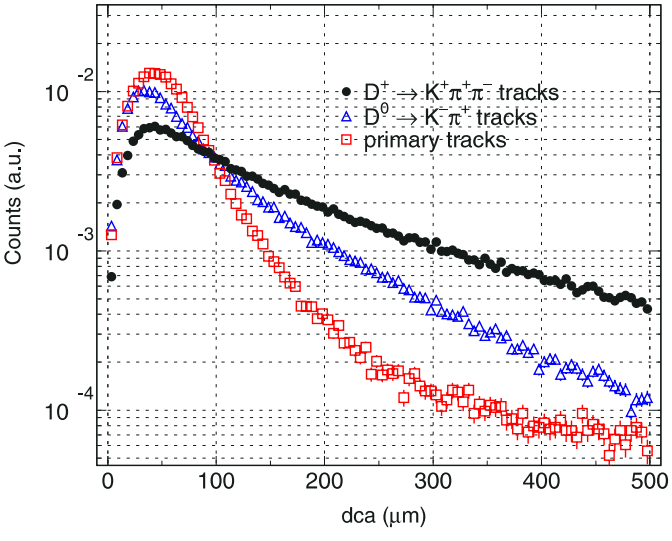

Fig. 3. The distance of closest approach (dca) distributions for D^0 (*triangles*) and D^+ (*circles*). The results of the dca primary tracks dca (background) is shown by the *squares* (simulation with TPC+SSD+HFT detectors included

2.2 Choice of technology: monolithic active pixel sensors

Silicon detectors are extensively used in many fields of experimental physics. Microstrip detectors were first used in vertex detectors. High precision unambiguous tracking is required by experiments. This triggered the development of pixel devices, offering a higher precision and replacing strip detectors when high precision is needed.

Three pixel technologies are available to modern experiments. The oldest one, charge coupled devices (CCDs), was proposed at the beginning of the 1980s and successfully used for construction of the vertex detector for the Stanford Linear Accelerator Center (SLAC) linear collider detector and under development for future international linear collider project. Hybrid pixel sensors (HPSs) developed for the Large Electron Positron 2 (LEP2) experiments are used by all large hadron collider (LHC) detectors, and especially the heavy ion one called A Large Ion Collider Experiment (ALICE).

Both CCDs and HPSs are high performance devices, but their balance between granularity, material budget, radiation tolerance and readout speed, is not well suited to take full advantage of experimental conditions met at STAR.

We propose to use a new technique, based on the commercial CMOS process, combining advantages of both CCDs and HPSs. They were developed for visible light imaging (e.g. commercial camcorders). Unlike HPSs, monolithic active pixel sensors [15] (MAPS) provide a high spatial resolution: their sensitive volume (epitaxial layer) is 10 to 20 μm thick. CMOS sensor can then be thinned down (like CCDs) to 30–50 μm. As granular as CCDs, they are faster.They also exhibit significantly better performance in terms of radiation tolerance. Additionally, signal processing circuits are fully integrated on the sensors substrate (system-on-chip). This allows for a compact and flexible architecture. CMOS is a standard, mass production fabrication technology, which allows for a reasonably cheap and fast turn-over for prototyping.

2.2.1 MAPS: Principle of operation

As illustrated by Fig. 4, the incoming particle produces an excess of charge carriers in the epitaxial layer at a rate of about 50 electron–hole pairs per micron [16].

Electron–hole pairs are produced along the particle track and diffuse thermally inside the epitaxial layer, which is located between two highly dopped zones: the substrate and the p-well diodes. The dopping level of the latter is three orders of magnitude higher than that of the epitaxial layer. This difference creates some kinetic potential 'barriers' at the boundaries, forcing the excess of e^- to remain inside the epitaxial layer. Subsequently, they are collected by some of the regularly implanted n-well diodes.

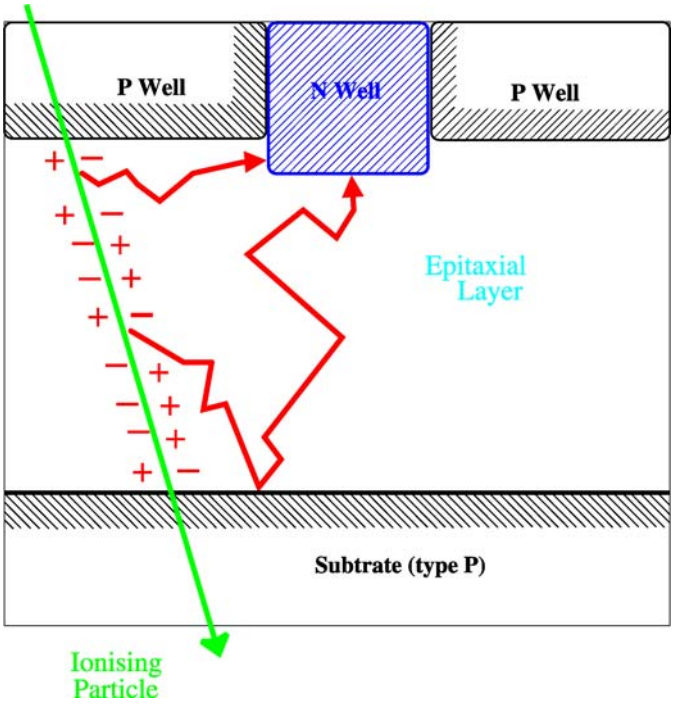

Fig. 4. Principle of operation of a CMOS sensor used for particle tracking. A single CMOS pixel is shown (sensitive element of the CMOS process)

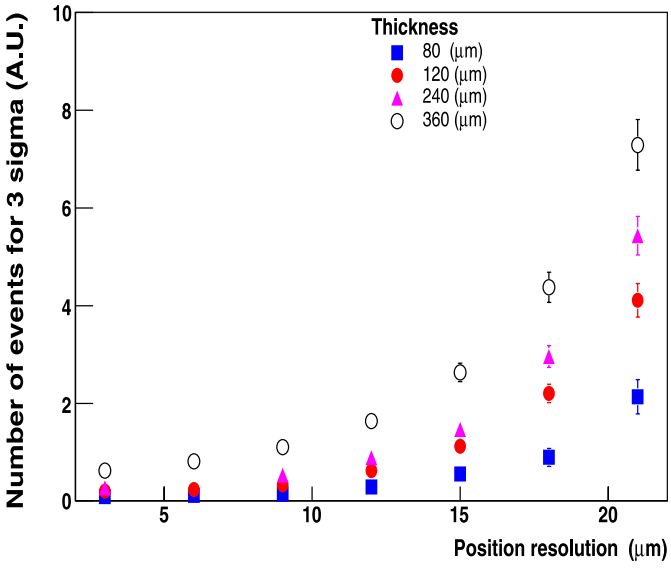

Fig. 5. Effects of the detector position resolution (x-axis) and of layer thickness (one curve per Si equivalent layer thickness) on detector performance (here the number of events needed to have a D^0 signal with a significance ≥ 3)

2.2.2 Current prototype: Mimo⋆ performances

The current CMOS sensor prototype called Mimo⋆ 2 is built and tested at IPHC. It is based on the AMS 0.35 μm opto. process, has 128×64 pixels (30 μm pitch) and is using an analogue readout (4 ms readout time with a 50 MHz pixel clock). The final HFT chips will be bigger with 640 pixels in a row $\times$ 320 column (with the same pitch).

This prototype has been tested in the DESY electron beam. At $T = 25\,^{\circ}\mathrm{C}$ and a read-out time of both 0.8 and 4 ms, the main results are: Noise 12–14e^- ENC (equivalent noise charge). The signal to noise ratio is varying between 15 and 21. The single point resolution is $\simeq 3\,\mu$m. The sensor efficiency is $\geq 99.8\%$. Its power dissipation is $40\,\mathrm{mW/cm^2}$.

Thanks to those tests, the architecture of the final prototypes sensor (Mimo⋆ 4) is validated (running conditions and temperature) and the design of the next one (Mimo⋆ 3) can start.

2.3 Effects of multiple Coulomb scattering and detector resolution

From simulation results presented Fig. 5 (see Sect. 3 for details): if the detector is too thick the tracking precision goes down and degradations, mainly caused by multiple Coulomb scattering (MCS), start to become significant. On the other hand, if the MCS contribution is large, there is no benefit to have a good intrinsic detector resolution. From this plot we can see that when using a detector resolution $\leq 10\,\mu$m and a thin enough detector layers (≤ 240–$360\,\mu$m equivalent Si per layer), the detector performance stays stable. In this region, the tracking is not too much affected by multiple scattering and the detector position resolution is good enough.

To obtain such a ladder thickness, our mechanical design makes significant use of carbon composite material, which has nearly the same radiation length as beryllium. In addition, as seen in Sect. 2.1, CMOS sensors single point resolution is small enough to meet our requirements.

2.4 Data acquisition

The proposed data acquisition system will have to be able to handle $100\,\mathrm{hits/cm^2}$ for the inner layer and $20\,\mathrm{hits/cm^2}$ for the outer one (at a machine luminosity of $10^{27}\,\mathrm{cm^{-2}\,s^{-1}}$). At these rates, the final average event size (on disk) is planned to be $\simeq 90$ kB. This will correspont to a data rate of about 90 MB/s with triggering rate of 1 kHz.

3 Detector simulations

The simulated geometry is, in the current design, composed of the HFT which is surrounded by one layer of silicon strips (the SSD [13]) itself surrounded by the STAR TPC [14].

Central Au + Au collisions at $\sqrt{s_{NN}} = 200\,\mathrm{GeV}$ are simulated in the STAR software framework. First, particles are produced by the MEVSIM [17] code. Then they are propagated through the detector material using GEANT, which parametrizes their interactions in detectors and supporting structures of the experiment. Detailed response simulations for the TPC and for the Silicon Drift Detector (SSD) were applied. This simulates the digitization

and the response of detector electronics. For the HFT, we smeared the position of the Monte Carlo hits using a Gaussian distribution with a sigma of 6 μm. Tracks are finally reconstructed using the new STAR tracking software package called Integrated Task Tracking Force [18] (ITTF).

The 4 ms read-out speed of the 1st generation HFT will lead to pile-up of 120 Au + Au collisions in the HFT at four times the RHIC design luminosity. We account for this by randomly uploading hits on top of the Monte Carlo generated hits in the HFT.

The STAR vertex finder package uses tracks defined with only the TPC and SSD to determine a primary vertex. We use a vertex constraint to improve the reconstruction efficiency and track matching purity: with the standard STAR algorithm, the tracker follows a series of hits in the TPC and SSD, refitting after every new hit is added. These tracks are then passed to the vertex finder, which reconstructs the event vertex. The tracks are extended to the resulting reconstructed vertex and, if the fit is successful, the new track is stored. The new algorithm simply takes these tracks and refits the track, this time with the HFT hits available. HFT hits that meet the tracking selection criteria are added. The Kalman fitter updates the track fit as the new HFT hits are added. The tracks with added HFT hits are then stored. The performance of this algorithm is dependent on the collision centrality. The vertex resolution follows the functional form: $\sigma = \frac{380\ \mu\mathrm{m}}{\sqrt{N_{\mathrm{ch}}}}$ where N_{ch} is the multiplicity of charged particles in the detector acceptance A vertex resolution of 8 μm was achieved for the highest multiplicity events.

The tracking efficiency obtained using the above vertex constraint technique, is $\simeq 45\%$ at $p_{\mathrm{T}} \sim 1\,\mathrm{GeV}/c$ and $\simeq 60\%$ at $p_{\mathrm{T}} \sim 3\,\mathrm{GeV}/c$. Candidate tracks in the HFT have TPC and SSD efficiencies and acceptance folded in.

Figure 6a compares the efficiency for D^+ reconstruction with the efficiency for reconstructing the two-body decay of D^0 and Fig. 6b shows the efficiency for reconstructing the three body-decays of D_s^+. The Λ_c baryon has also been studied, but is not discussed here.

In the present article, we will focus on the D^0 meson reconstruction and v_2.

The HFT detector is designed to allow us to identify a D^0 decay by reconstructing its secondary (displaced) vertex ($D^0 \to K\pi$, $c\tau = 123\ \mu$m).

The following selection variables were used to identify $D^0 s$: the decay length l (distance between the primary vertex and the displaced-vertex). The distance of closest approach $\mathrm{DCA_{KP}}$, between the two daughter tracks at the secondary vertex. In addition two opening angle cuts where used: the first one is on $\cos\theta$ (angle between the vector sum of the two daughter momenta and the vector joining the primary vertex to the D^0 secondary vertex). The last uses $\cos\theta\star$, which is the same angle, but in the D^0 center of mass frame.

Charged decay daughters were identified using their amount of energy lost in the TPC gas and the time of flight measured in the TOF. For example, to identify pions, we used a 3σ cut around the expected $\mathrm{d}E/\mathrm{d}x$ band for pions. Using the TPC pions can be separated from kaons up to 700 MeV/c. The TOF detector extends this range up to 1.6 GeV/c, as demonstrated from existing STAR data [19]. Tracks with a momentum above the range of these particles identification (PID) methods can still be used, but they must be entered into the reconstruction algorithm twice, once under a pion mass assumption and once assuming a kaon mass.

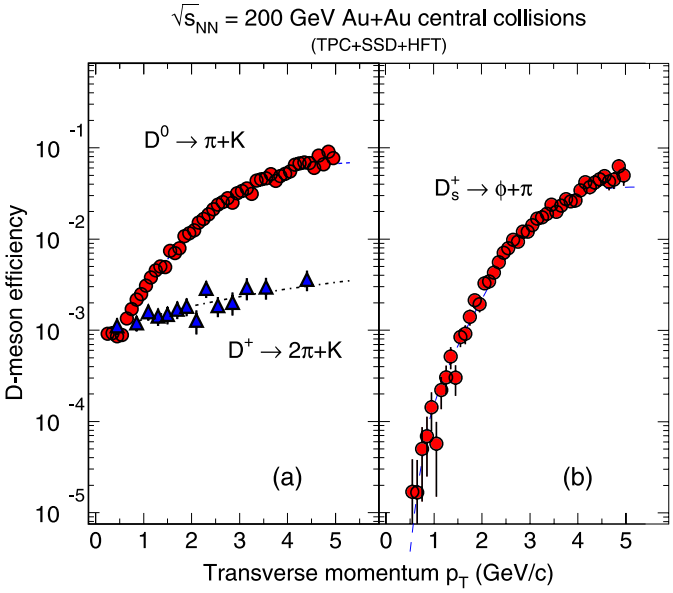

Fig. 6. Summary of the HFT D-meson reconstruction efficiencies ($\epsilon = \frac{N_{\mathrm{Reconstructed}}}{N_{\mathrm{MC,Accepted}}}$) as a function of transverse momentum. The D^0 efficiency saturates at 10%, while the D^+ efficiency approaches 0.3%

The optimization of the reconstruction cuts is important, to obtain a good signal over noise ratio, keep the background reasonably low and find a good balance between efficiency and purity.

The D^0 reconstruction cuts parameters were determined by using three different techniques: The first one is the usual one where cuts are hand-tuned sequentially and applied on the reconstructed variables presented above. As a quite large number of systematic studies were required to study the detector performances (for instance Fig. 5), we started to use the minimization program MINUIT. The variable $S/\sqrt{S+B}$ often called significance was used as the variable to maximize [20]. This algorithm returns a set of cuts, from witch the final set is chosen after making sure not to have found a local minimum. The last method (not discussed in the present article), is based on using a neural network to find good selection criteria. Figure 7 shows how the D^0 invariant mass is modified (and how the signal to background ratio changes), as the cuts are being optimized. With the best set, the background is small and the signal/background $\simeq 3$. As opposed to what needs to be done using the event-mixing technique (without the HFT), no specific background suppression technique is needed here. A reliable subtraction of the background is possible leading to small systematic uncertainties.

The reconstruction efficiency obtained is shown in Fig. 8. The efficiency takes into account acceptance, single

track efficiency and reconstruction efficiency (with our best set of cuts). We have studied the D^0 detection efficiency in three cases: assuming a perfect knowledge of the location of the primary vertex, a resolution of 20 μm on the vertex and a thicker configuration assuming 1000 μm Si equivalent per layer (instead of 360 μm), which is similar to the thickness of the ALICE silicon detector. The overall reconstruction efficiency increases with increasing momentum and saturates above 3 GeV/c at a value of about 10%. In the thicker case the efficiency is about 8 times less. This demonstrates again the influence of the detector thickness on the physics performances.

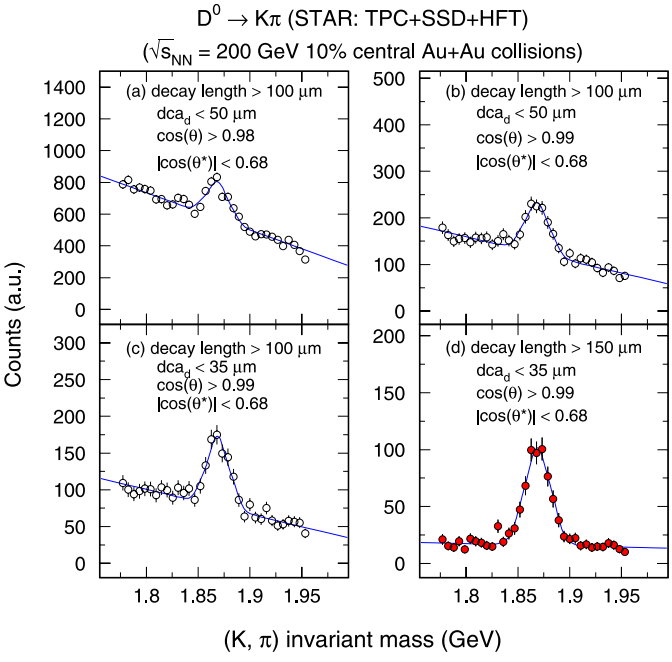

Fig. 7. D^0 invariant mass peaks. Each *panel* corresponds to a different cut set. As the cuts are optimized, the background is reduced and the signal significance improved

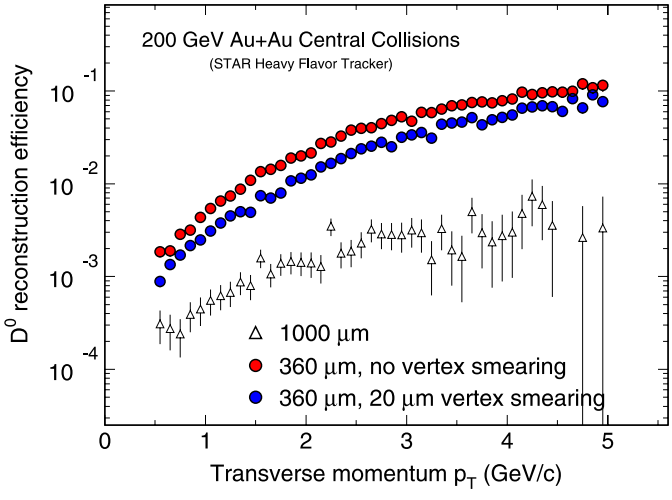

Fig. 8. D^0 reconstruction efficiency using TPC+SSD+HFT as function of transverse momentum. For comparison purposes, a simulation with thicker Si layers is also shown (1000 μm equivalent silicon thickness per layer)

3.1 Estimation of the rates

As discussed in Sect. 1, a measurement of charm elliptic flow is important. The measurement may help us understand the degree of thermalization in the partonic phase of a relativistic collision. To study the sensitivity of the HFT for such a measurement, we focused on the capability of the HFT to measure the elliptic flow of D^0 mesons. The simulated D^0 transverse momentum distribution was generated from 200 GeV $p+p$ collisions in Pythia. The spectral shape follows a power-law distribution and the integrated yield is fixed to the yield measured [7, 8] at mid-rapidity at RHIC, or $\mathrm{d}N/\mathrm{d}y = 0.03$. The default value of $\mathrm{d}N/\mathrm{d}y$ in Pythia is about a factor of 3 lower. For the 10% most-central and 0–80% minimum bias Au + Au collisions, the average number of binary collisions are 950 and 290 respectively. Requiring 10% statistical errors in each p_T bin, the number of events required can be easily calculated. At $p_\mathrm{T} \simeq 10$ GeV/c, a good R_{AA} measurement requires about 7.5 billion $p+p$ events and 10 million Au + Au 10% central events. These numbers are achievable with the planned RHIC luminosity, 60% duty factor and the current STAR detector system in a week of RHIC running. In order to make a rate estimate relevant for the charm v_2 measurement, we need to make further assumptions about the p_T dependence of the anisotropy. Models of D^0 flow with and without charm quark flow, represent the extreme cases and thus the expected measurement range. With these assumptions and the known reconstruction efficiency, the rates can be estimated. Using the proposed HFT, the D^0 v_2 can be measured with a relative statistical uncertainty lower than 10% up to a p_T of 5 GeV/c with 500 millions of events. Considering that 50 million Au + Au events were taken during STAR run IV and that RHIC luminosity will increase, this 500 million events could be taken during the first HFT running cycle.

4 Summary

In order to address open questions (discussed in Sect. 1), we need a device able to achieve direct topological reconstruction of charm decays. A precise measurements of charm mesons and baryons and their ratio may allow us to look for manifestations of the coalescence model (seen with light quarks), in the charm sector.

The proposed HFT seems a good candidate and is being designed to be very thin ($\simeq 0.28\% X_0$ of radiation length per layer), precise ($\simeq 10\,\mu$m) and to use the CMOS technology (see Sect. 2). Using such a device, charm spectra, angular correlations, R_{AA} and R_CP, measurements will become accessible.

A full scale prototype is planned to be operational in STAR in 2009. The ultimate HFT detector (a faster version of the above, able to handle RHIC2 luminosity) is planned for 2011.

References

1. STAR Collaboration, C. Adler et al., Phys. Rev. Lett. **90**, 082 302 (2003)
2. J. Adams et al., Phys. Rev. Lett. **95**, 122 301 (2005)
3. U. Heinz, P.D.F. Kolb, Nucl. Phys. A **702**, 269 (2002)
4. S. Eidelman et al., Phys. Lett. B **592**, 1 (2004)
5. STAR Collaboration, B.I. Abelev et al., nucl-ex/0607012 (2006)
6. K.H. Ackermann et al., Nucl. Instrum. Methods A **499**, 624 (2003)
7. J. Adams, et al., Phys. Rev. Lett. **94**, 062 301 (2005)
8. STAR Collaboration, H. Zhang et al., nucl-ex/0510063 (2005)
9. STAR Collaboration, Y. Zhang, nucl-ex/0607011 (2006)
10. S.A. Butsyk, nucl-ex/0510010 (2005)
11. M. Djordjevic, nucl-th/0603066 (2006)
12. Z. Xu et al., LBNL-PUB-5509 (2006)
13. L. Arnold et al., Nucl. Instrum. Methods A **499**, 652 (2003)
14. M. Anderson et al., Nucl. Instrum. Methods A **499**, 659 (2003)
15. M. Winter et al., Nucl. Instrum. Methods A **560**, 44 (2006)
16. H. Bichsel, Nucl. Instrum. Methods A **562**, 154 (2006)
17. R.L. Ray, R.S. Longacre, STAR note 419
18. STAR Collaboration, A. Rose et al., nucl-ex/0307015 (2003)
19. STAR Collaboration, J. Adams et al., Phys. Lett. B **616**, 8 (2005)
20. http://www.star.bnl.gov/∼shabetai